Inorganic Chemistry

Article

pubs.acs.org/IC

Novel Synthesis and Structural Analysis of Ferrihydrite

Stacey J. Smith,[†,‡] Katharine Page,[§] Hyunjeong Kim,[§] Branton J. Campbell,[‡] Juliana Boerio-Goates,[†] and Brian F. Woodfield*[,†]

[†]Brigham Young University, Chemistry & Biochemistry, Provo, Utah 84602, United States

[‡]Brigham Young University, Physics & Astronomy, Provo, Utah 84602, United States

[§]Lujan Neutron Scattering Center, Los Alamos National Laboratory, Los Alamos, New Mexico 87545, United States

ABSTRACT: Naturally occurring ferrihydrite is both impure and difficult to isolate, so the numerous applications and interesting properties of ferrihydrite have spurred the development of various synthetic techniques. Nearly all techniques are based on the hydrolysis of an iron salt and require careful control of temperature, pH, and concentration. In this Article, we report a new synthetic method which does not require such control and is perhaps the fastest and simplest route to synthesizing ferrhydrite. XRD, TEM, BET, and chemical purity characterizations show that the chemically pure, 2-line ferrihydrite product consists of crystallites 2−6 nm in diameter which aggregate to form mesoporous, high surface area agglomerates that are attractive candidates for the many adsorption applications of ferrihydrite. X-ray PDF data were also collected for the ferrihydrite product and refined against the hexagonal structural model recently proposed by Michel et al. These analyses suggest that ferrihydrite has a consistent, repeatable structure independent of variation in the synthetic method, water content of the sample, or particle size of the crystallites, and this structure can be adequately described by the proposed hexagonal model.

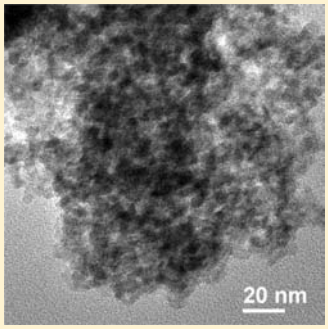

INTRODUCTION

Ferrihydrite is a poorly crystalline Fe(III) oxyhydroxide mineral naturally found in near-surface soils and sediments as the precursor to hematite, often in areas contaminated by acid mine drainage.[1−4] It has a number of useful properties. The high surface area and reactivity of ferrihydrite enable it to sequester various species through adsorption, coprecipitation, and redox reactions.[5] It is a particularly effective sorbent for heavy metals[6] and arsenate[7] and is thus manufactured for use in wastewater treatment,[8] direct coal liquefaction,[9] and metallurgical processing.[9,10] Its adsorptive nature is also being explored for use in removal of volatile organic compounds from the air.[11] Electronically, ferrihydrite displays quantum dot behavior because its band gap varies from 1.3 to 2.5 eV as particle size varies from 2 to 8 nm.[12] It is also thought to be the structure formed in the iron core of ferritin, an iron storage protein ubiquitously found in animals, plants, and microbes.[4,13,14]

Naturally occurring ferrihydrite is both impure and difficult to isolate;[15] thus, its applications and interesting properties have spurred the development of new synthetic techniques.[8,11,16−18] All are essentially variations on the hydrolysis of an iron salt. For example, a common synthetic route involves the titration (at numerous different rates) of an aqueous Fe(III) solution with a base at a controlled temperature (often either 25 °C or 65−85 °C) to either achieve a neutral pH (usually 6.5−7.5) or maintain a specific acidic pH (roughly 2.65) until either a precipitate forms or the solution is quenched to cooler temperatures to induce precipitation. Virtually all reported synthetic processes require careful control over temperature, pH, concentration, and the rate of change in these variables, and all require subsequent washing/dialysis and drying steps to remove residual electrolytes.

In this Article, we report a new method for synthesizing ferrihydrite which does not require careful control over temperature, pH, concentration, or the rate of change in these variables and is therefore the simplest method reported thus far. The distinctive feature of the synthesis is the solvent-deficient environment[19−21] in which the particles form which results in unusually low water content in the ferrihydrite. X-ray diffraction (XRD), transmission electron microscopy (TEM), Brunauer−Emmett−Teller (BET), and chemical purity characterizations of our ferrihydrite product are presented, along with synchrotron X-ray pair-distribution function (PDF) data that has been analyzed using the structural model recently proposed by Michel et al.[1] These analyses suggest that ferrihydrite has a consistent, repeatable structure independent of variation in synthetic method, water content of the sample, or particle size of the crystallites, and this structure can be adequately described by the proposed hexagonal model.

EXPERIMENTAL METHODS

Synthesis. Our ferrihydrite synthesis was derived from the solvent-deficient method recently reported for the synthesis of metal oxide nanoparticles[19−21] with the primary alteration being that drying and rinsing steps were employed in lieu of the calcination step used in that method. Our ferrihydrite synthesis thus has four simple steps: (1) grinding, (2) drying, (3) rinsing, and (4) drying. First, $Fe(NO_3)_3{\cdot}9H_2O(s)$ and $NH_4HCO_3(s)$ in a 1:3 mole ratio are ground

Received: May 7, 2012
Published: May 22, 2012

   dx.doi.org/10.1021/ic300937f | *Inorg. Chem.* 2012, 51, 6421−6424

together using a mortar and pestle. The grinding action dislodges the waters of hydration from the metal salt, providing sufficient solvent for the reagents to begin dissociating. The metal cations acidify the solution, causing the bicarbonate to decompose into CO_2 gas and H_2O. The decomposition of the bicarbonate to form additional H_2O begins a chain reaction of dissociation and decomposition that produces visible bubbles in the rapidly forming liquid. Grinding continues until bubbling ceases and a dark brown precipitate has formed.

The resulting slurry is then dried in air between 80 and 100 °C. The dried precipitate is rinsed to remove the NH_4NO_3 salt that forms as the precursor is dried. Only 2−3 washings on the vacuum filter using distilled water are necessary; we have found that the ferrihydrite can transform to goethite if it is allowed to sit in water for extended periods of time or if the precipitate is rinsed before being dried. The reddish-brown precipitate is then dried again in air as before.

For the characterizations discussed herein, a ferrihydrite sample was produced by grinding 20.252 g of $Fe(NO_3)_3{\cdot}9H_2O(s)$ (0.050 12 mol) with 11.913 g of $NH_4HCO_3(s)$ (0.1507 mol) for roughly 15 min using a mortar and pestle. The resulting slurry was dried in air at 100 °C for 24 h before being rinsed using three 50 mL portions of distilled water. The remaining precipitate was then dried in air at 100 °C for 24 h. The elemental nitrogen and hydrogen content in the ferrihydrite were determined via combustion analysis by Galbraith Laboratories in order to gauge the effectiveness of rinsing away the NH_4NO_3 impurity. The nitrogen content was found to be less than 0.5 mass %, which is below the detection limit for the combustion technique. The hydrogen analysis was also used to estimate the water content of the ferrihydrite sample.

Structural Characterization. A laboratory X-ray powder diffraction (XRD) pattern of the ferrihydrite sample was collected over a 10−90° 2θ range in 0.016° steps at a rate of 3 s/step using a PANalytical X'Pert Pro diffractometer with a Cu source, a Ge 111 Johanssen-type monochromator tuned to the Cu−$K_{\alpha 1}$ wavelength (λ = 1.540 598 Å), and an X'Celerator position-sensitive detector.

High-resolution transmission electron microscope (HRTEM) images were recorded using a FEI Philips Technai F30 TEM operating at 300 kV. Specimens were prepared by dispersing the particles in ethanol, placing a drop of the very dilute solution on a Formvar/carbon film supported by a 200 mesh Ni grid (Ted-Pella Inc.), and allowing the ethanol to evaporate. Mass/thickness contrast images were recorded in standard high-resolution mode.

BET specific surface area and pore size were determined from N_2 adsorption at 77 K using a Micromeritics TriStar II instrument. For these measurements, 0.2149 g of ferrihydrite was degassed at 200 °C for 22 h and then allowed to cool to room temperature prior to data collection.

High-energy X-ray total scattering data for PDF (pair distribution function) analysis were collected under ambient conditions at the 11-ID-B beamline at the Advanced Photon Source (APS) at Argonne National Laboratory. Approximately 10 mg of ferrihydrite powder were loaded into a 0.0395 in. inner-diameter polyimide capillary that was sealed with epoxy at both ends. Using 90.4868 keV (λ = 0.1370 Å) incident-energy X-rays, a 2-D image of the diffraction data was collected out to a maximum value of Q = 39 $Å^{-1}$ with a 2048 × 2048 pixel Perkin-Elmer (PE) amorphous-silicon area detector of square dimension 410 cm. The Fit2D[22] and PDFgetX2[23] software packages were used to integrate the 2D ring patterns and extract the experimental PDF pattern, $G(r)$.[24] Structural model refinements against the PDF data were performed with the PDFgui software[25] in the range from r = 1.6 to r = 20.00 Å.

The Fhyd6 structure reported by Michel et al.[1] was used as the initial model in the PDF refinement. The unit cell parameters, atom positions, isotropic-displacement parameters, and occupancies of the second and third Fe atoms (Fe2 and Fe3) were refined. A number of PDF-specific parameters were also refined, including the data scale factor, the *Qdamp* resolution-damping parameter, and the *sratio* parameter (with *rcut* set to 4.0 Å) which was added to model the sharpening of nearest-neighbor peaks due to correlated atomic motion. The *Qdamp* parameter was used to account for both instrument resolution and finite particle size effects (instead of refining a separate spherical shape factor to account for the size effects) in order to make the parameters comparable to those reported by Michel et al.

RESULTS AND DISCUSSION

XRD patterns reported for ferrihydrite typically display either two or six broad and poorly defined reflections, which is the

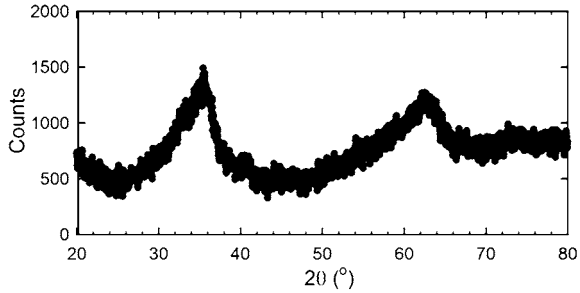

Figure 1. XRD pattern of the 2-line ferrihydrite synthesized via our solvent-deficient method.

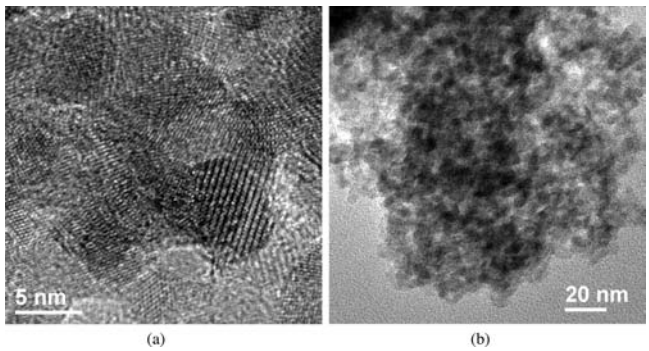

Figure 2. TEM images of ferrihydrite synthesized via our solvent-deficient method.

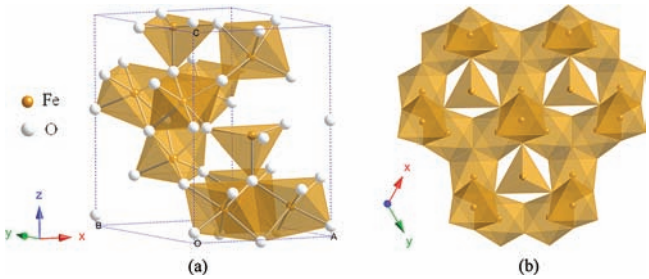

Figure 3. (a) Unit cell and (b) basic motif of the ferrihydrite structure proposed by Michel et al.[1].

source of the common practice of designating the compound as either 2-line or 6-line ferrihydrite.[1,4] As evidenced by the two very broad diffraction peaks in Figure 1, our solvent-deficient synthetic method produces 2-line ferrihydrite. The distinction between 2-line and 6-line ferrihydrite is somewhat artificial, however. Structurally, the two are quite similar, as Carta et al. recently demonstrated using X-ray absorption near edge structure (XANES)/extended X-ray absorption fine structure (EXAFS).[15] The primary difference lies in the size of their coherent scattering domains[26] or crystal sizes; the broad peaks of 2-line ferrihydrite actually resolve smoothly into the slightly sharper reflections of 6-line ferrihydrite as the rate of hydrolysis is slowed and crystallinity increases.[17,27] We have found that the

dx.doi.org/10.1021/ic300937f | Inorg. Chem. 2012, 51, 6421−6424

Table 1. Ferrihydrite Structural Parameters Obtained from PDF Refinements[a]

	a	*c*	*Qdamp*	R_w (%)	*sratio*
this work	5.949	8.992	0.157	24.0	0.521
Fhyd2	5.958	8.965	0.217	26.2	0.336
Fhyd3	5.953	9.096	0.157	24.9	0.406
Fhyd6	5.928	9.126	0.137	26.7	0.400

	this work				Michel et al.'s work			
atom	*x*	*y*	*z*	*Occ*	*x*	*y*	*z*	*Occ*
Fe1 (6c)	0.16986	0.8302	0.6361	1.0	0.1688-95	0.8304-12	0.6356-0.6365	1.0
Fe2 (2b)	1/3	2/3	0.3359	0.94	1/3	2/3	0.3347-0.3414	0.90-97
Fe3 (2b)	1/3	2/3	0.9605	0.87	1/3	2/3	0.9538-0.9600	0.85-96
O1 (2a)	0	0	0.0503	1.0	0	0	0.0147-0.0460	1.0
O2 (2b)	1/3	2/3	0.7470	1.0	1/3	2/3	0.7353-0.7651	1.0
O3 (6c)	0.1650	0.8350	0.2487	1.0	0.1670-97	0.8302-29	0.2457-0.2547	1.0
O4 (6c)	0.5263	0.4737	0.9861	1.0	0.5227-58	0.4742-73	0.9778-0.0053	1.0

[a]Shown in comparison are the parameters of Michel et al.'s three samples (Fhyd 2, 3, and 6). To conserve space, only the range of values is given for the atomic coordinates and occupancies of the three samples.

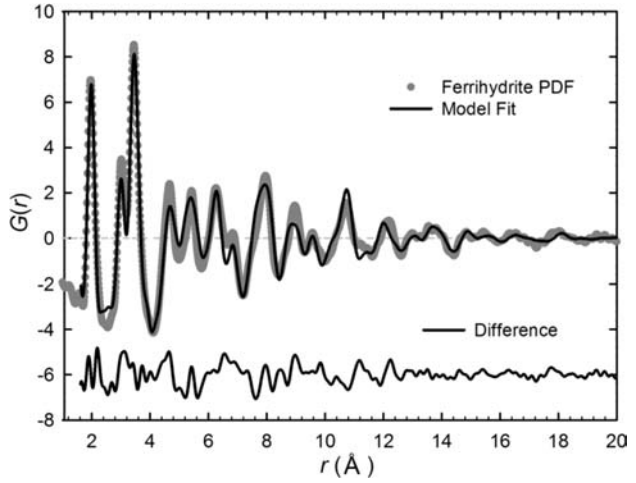

Figure 4. Experimental PDF, or $G(r)$, of the ferrihydrite (gray) with the refined fit of the model (black). The difference plot is shown below.

synthetic method reported here cannot be slowed or extended sufficiently to produce the more crystalline 6-line ferrihydrite; only 2-line ferrihydrite can be produced due to the rapid reaction rate and poor mass transport of the reagents in the solvent-deficient environment.

The small crystallites sizes (approximately 2−6 nm) of the 2-line ferrihydrite particles are shown in the TEM images of Figure 2a, which also reveal the roughly spherical morphology of the particles. These small particles aggregate to satisfy the high surface energies characteristic of nanoparticles,[28] forming the agglomerates illustrated in Figure 2b whose BET surface area is 248 m^2/g and whose pores are 3.4 nm in diameter and 0.26 cm^3/g in volume. Considering this large surface area, the ferrihydrite exhibits surprisingly low adsorbed water content. Because the undetectable (<0.5 mass %) nitrogen content implies that the sample does not contain any residual NH_4NO_3, the hydrogen content (1.09 mass %) from the Galbraith analyses can be attributed solely to either hydroxide anions or excess water. Assuming the chemical formula $Fe_{10}O_{14}(OH)_2{\cdot}xH_2O$ for ferrihydrite suggested by Michel et al.,[1] the value of x for this sample is 3.8 (or else $x \approx 0$ for the commonly used chemical formula $FeOOH{\cdot}xH_2O$). Compared to precipitation methods, which typically report $x \approx 8$ ($x \approx 0.4$ for $FeOOH{\cdot}xH_2O$), the ferrihydrite synthesized via the solvent-deficient method has less than half the typical water content.[1,4] We presume that this is a result of the oxyhydroxide's limited access to water in the solvent-deficient synthetic environment. Presuming it enables the ferrihydrite to be a more effective sorbent, however, this low water content could be highly advantageous. Combined with the excellent chemical purity, high surface area, and naturally mesoporous nature of the agglomerates, the ferrihydrite produced by our solvent-deficient method is an attractive candidate for adsorption applications.

The TEM images in Figure 2 also display conspicuous lattice fringes which confirm the crystalline nature of the particles despite their small size and poorly defined diffraction pattern. Notwithstanding the obvious crystallinity of the particles and the considerable attention ferrihydrite has received, studies and discussions continue to debate both its structure and its chemical formula.[1,14,15,26,27,29−32] No single chemical formula has been accepted because of the variable water content commonly observed in ferrihyrite,[4] and a definitive structural model is evasive because the nanocrystallinity (2−8 nm) of ferrihydrite stymies traditional crystallographic analyses which rely on long-range order.

Even so, several structural models have been proposed for ferrihydrite over the years. Chukrov et al.[32] and Towe and Bradley[14] both proposed defective hematite structures. Drits et al. proposed a multicomponent model consisting of defective and defect-free ferrihydrite phases mixed with ultradisperse hematite.[31] More recently, Michel et al. employed the PDF method of analyzing total scattering data to propose a single-phase hexagonal structure with $P6_3mc$ symmetry and average unit cell dimensions of a = ∼5.95 Å and c = ∼9.06 Å (Figure 3a) that successfully reproduced the X-ray PDFs of three different samples of ferrihydrite (2, 3, and 6 nm in size).[1] The basic unit of their structure is similar to a δ-Keggin cluster[33] and consists of a central tetrahedrally coordinated Fe atom sharing each of its corners with three edge-sharing Fe octrahedra (Figure 3b). Since then, XANES/EXAFS studies by both Carta et al.[15] and Maillot et al.[30] have supported the 20:80 ratio of tetrahedrally and octrahedrally coordinated Fe atoms in ferrihydrite suggested by Michel et al.'s model.

To determine the structural similarities or differences between the less-hydrated ferrihydrite synthesized via our solvent-deficient method and ferrihydrite reported elsewhere, we collected PDF data on our ferrihydrite sample and used

dx.doi.org/10.1021/ic300937f | Inorg. Chem. 2012, 51, 6421−6424

Michel et al.'s structure as a starting model for a refinement. The refinement results, which appear in Table 1 and Figure 4, indicate that the structural parameters of our ferrihydrite sample generally fall within the ranges of those reported for Michel et al.'s three samples. The small discrepancies between our experimental and the calculated PDF peak heights, particularly those at 3.0, 4.6, 6.8, 8.9, and 10.7 Å, were also present in the previous study, wherein they were rationalized by noting their similarity to stacking-fault induced misfits in studies of Al_2O_3.[34] The PDF data and refined models of the four samples are thus essentially identical despite the materials having been synthesized by four different methods and despite the differences in particle size and water content. (The water contents of the other three samples were not reported, but we presume they are similar to those reported by other precipitation methods.)

CONCLUSION

We conclude that our simple, solvent-deficient synthetic method produces chemically pure ferrihydrite crystallites 2−6 nm in size whose agglomerates are good candidates for adsorption applications due to their high surface areas, mesoporous nature, and unusually low water content. The ferrihydrite product is also virtually identical in structure to that produced by other synthetic methods which require very careful control over temperature, pH, concentration, and the changes in these variables. This result implies that the ferrihydrite material has a consistent, repeatable structure independent of variation in synthetic method, water content of the sample, or particle size of the crystallites, and the structure is adequately described by the hexagonal model proposed by Michel et al.

AUTHOR INFORMATION

Corresponding Author

*E-mail: Brian_Woodfield@byu.edu.

Notes

The authors declare no competing financial interest.

ACKNOWLEDGMENTS

Use of the Advanced Photon Source at Argonne National Laboratory was supported by the U.S. Department of Energy, Office of Science, Office of Basic Energy Sciences, under Contract No. DE-AC02-06CH11357. Other funding for this work was provided by the U.S. Department of Energy under Grant DE-FG02-05ER15666 and the National Science Foundation under CHE-0959862.

REFERENCES

(1) Michel, F. M.; Ehm, L.; Antao, S. M.; Lee, P. L.; Chupas, P. J.; Liu, G.; Strongin, D. R.; Schoonen, M. A. A.; Phillips, B. L.; Parise, J. B. *Science (Washington, DC, U. S.)* **2007**, *316*, 1726−1729.

(2) Rancourt, D. G.; Fortin, D.; Pichler, T.; Thibault, P.-J.; Lamarche, G.; Morris, R. V.; Mercier, P. H. J. *Am. Mineral.* **2001**, *86* (7−8), 834−851.

(3) Schwertmann, U.; Carlson, L.; Murad, E. *Clays Clay Miner.* **1987**, *35* (4), 297−304.

(4) Jambor, J. L.; Dutrizac, J. E. *Chem. Rev.* **1998**, *98* (7), 2549−2585.

(5) Fortin, D.; Langley, S. *Earth-Sci. Rev.* **2005**, *72* (1−2), 1−19.

(6) Ford, R. G.; Bertsch, P. M.; Farley, K. J. *Environ. Sci. Technol.* **1997**, *31* (7), 2028−2033.

(7) Raven, K. P.; Jain, A.; Loeppert, R. H. *Environ. Sci. Technol.* **1998**, *32* (3), 344−349.

(8) Li, Z.; Zhang, T.; Li, K. *Dalton Trans.* **2011**, *40* (9), 2062−2066.

(9) Huffman, G. P.; Ganguly, B.; Zhao, J.; Rao, K. R. P. M.; Shah, N.; Feng, Z.; Huggins, F. E.; Taghiei, M. M.; Lu, F.; et al. *Energy Fuels* **1993**, *7* (2), 285−296.

(10) Riveros, P. A.; Dutrizac, J. E.; Spencer, P. *Can. Metall. Q.* **2001**, *40* (4), 395−420.

(11) Mathew, T.; Suzuki, K.; Nagai, Y.; Nonaka, T.; Ikuta, Y.; Takahashi, N.; Suzuki, N.; Shinjoh, H. *Chem.—Eur. J.* **2011**, *17* (4), 1092−1095−S1092/1-S1092/9.

(12) Liu, G.; Debnath, S.; Paul, K. W.; Han, W.; Hausner, D. B.; Hosein, H.-A.; Michel, F. M.; Parise, J. B.; Sparks, D. L.; Strongin, D. R. *Langmuir* **2006**, *22* (22), 9313−9321.

(13) Lewin, A.; Moore, G. R.; Le Brun, N. E. *Dalton Trans.* **2005**, *22*, 3597−3610.

(14) Towe, K. M.; Bradley, W. F. *J. Colloid Interface Sci.* **1967**, *24* (3), 384−92.

(15) Carta, D.; Casula, M. F.; Corrias, A.; Falqui, A.; Navarra, G.; Pinna, G. *Mater. Chem. Phys.* **2009**, *113* (1), 349−355.

(16) Anschutz, A. J.; Penn, R. L. *Geochem. Trans.* **2005**, *6* (3), 60−66.

(17) Schwertmann, U. F., J.; Kyek, A. *Clays Clay Miner.* **2004**, *52* (2), 221−226.

(18) Dyer, L.; Fawell, P. D.; Newman, O. M. G.; Richmond, W. R. *J. Colloid Interface Sci.* **2010**, *348* (1), 65−70.

(19) Woodfield, B. F.; Liu, S.; Boerio-Goates, J.; Liu, Q.; Smith, S. J. Preparation of uniform nanoparticles of ultra-high purity metal oxides, mixed metal oxides, metals, and metal alloys. 2007-US4279, 2007098111, 20070216, 2007.

(20) Smith, S. J.; Liu, S.; Liu, Q.; Olsen, R. E.; Boerio-Goates, J.; Woodfield, B. F. *Chem. Mater.* **2012**, submitted.

(21) Smith, S. J.; Liu, S.; Liu, Q.; Olsen, R. E.; Rytting, M.; Selck, D. A.; Simmons, C. L.; Boerio-Goates, J.; Woodfield, B. F. *Chem. Mater.* **2012**, Submitted.

(22) Fit2D V. 9.129 reference manual V. 3.1.

(23) Qiu, X.; Thompson, J. W.; Billinge, S. J. L. *J. Appl. Crystallogr.* **2004**, *37* (4), 678.

(24) Egami, T. B., S., J. L., *Underneath the Bragg Peaks: Structural Analysis of Complex Materials*; 1st ed.; Pergamon: Kidlington, Oxford, U.K., 2003; Vol. 7, p 404.

(25) Farrow, C. L.; Juhas, P.; Liu, J. W.; Bryndin, D.; Bozin, E. S.; Bloch, J.; Proffen, T.; Billinge, S. J. L. *J. Phys.: Condens. Matter* **2007**, *19* (33), 335219/1−335219/7.

(26) Kukkadapu, R. K.; Zachara, J. M.; Fredrickson, J. K.; Smith, S. C.; Dohnalkova, A. C.; Russell, C. K. *Am. Mineral.* **2003**, *88*, 1903−1914.

(27) Schwertmann, U.; Friedl, J.; Stanjek, H.; From, Fe(III *J. Colloid Interface Sci.* **1999**, *209* (1), 215−223.

(28) Nanda, K. K.; Maisels, A.; Kruis, F. E.; Fissan, H.; Stappert, S. *Phys. Rev. Lett.* **2003**, *91* (10), 106102/1−106102/4.

(29) Jansen, E.; Kyek, A.; Schafer, W.; Schwertmann, U. *Appl. Phys. A: Mater. Sci. Process* **2002**, *74* (Suppl., Pt. 2), S1004−S1006.

(30) Maillot, F.; Morin, G.; Wang, Y.; Bonnin, D.; Ildefonse, P.; Chaneac, C.; Calas, G. *Geochim. Cosmochim. Acta* **2011**, *75* (10), 2708−2720.

(31) Drits, V. A.; Sakharov, B. A.; Salyn, A. L.; Manceau, A. *Clay Miner.* **1993**, *28* (2), 185−207.

(32) Chukhrov, F. V.; Zvyagin, B. B.; Gorshkov, A. I.; Ermilova, L. P.; Balashova, V. V. *Izvestiya Akademii Nauk SSSR, Seriya Geologicheskaya* **1973**, *4*, 23−33.

(33) Casey, W. H. *Chem. Rev.* **2006**, *106* (1), 1−16.

(34) Paglia, G.; Bozin, E. S.; Billinge, S. J. L. *Chem. Mater.* **2006**, *18* (14), 3242−3248.